

Available online at [www.sciencedirect.com](http://www.sciencedirect.com)

Journal of Structural Biology xxx (2006) xxx–xxx

Journal of  
Structural  
Biology

[www.elsevier.com/locate/yjsbi](http://www.elsevier.com/locate/yjsbi)

## Mechanical properties of cardiac titin's N2B-region by single-molecule atomic force spectroscopy

Mark C. Leake<sup>a</sup>, Anika Grützner<sup>b</sup>, Martina Krüger<sup>b</sup>, Wolfgang A. Linke<sup>b,\*</sup>

<sup>a</sup> Clarendon Laboratory, University of Oxford, Parks Road, Oxford OX1 3PU, UK

<sup>b</sup> Physiology and Biophysics Unit, University of Muenster, Schlossplatz 5, D-48149 Muenster, Germany

Received 27 November 2005; accepted 20 February 2006

### Abstract

Titin is a giant protein responsible for passive-tension generation in muscle sarcomeres. Here, we used single-molecule AFM force spectroscopy to investigate the mechanical characteristics of a recombinant construct from the human cardiac-specific N2B-region, which harbors a 572-residue unique sequence flanked by two immunoglobulin (Ig) domains on either side. Force-extension curves of the N2B-construct revealed mean unfolding forces for the Ig-domains similar to those of a recombinant fragment from the distal Ig-region in titin (I91–98). The mean contour length of the N2B-unique sequence was 120 nm, but there was a bimodal distribution centered at ~95 nm (major peak) and 180 nm (minor peak). These values are lower than expected if the N2B-unique sequence were a permanently unfolded entropic spring, but are consistent with the ~100 nm maximum extension of that segment measured in isolated stretched cardiomyofibrils. A contour-length below 200 nm would be reasonable, however, if the N2B-unique sequence were stabilized by a disulphide bridge, as suggested by several disulphide connectivity prediction algorithms. Since the N2B-unique sequence can be phosphorylated by protein kinase A (PKA), which lowers titin-based stiffness, we studied whether addition of PKA (+ATP) affects the mechanical properties of the N2B-construct, but found no changes. The softening effect of PKA on N2B-titin may require specific conditions/factors present inside the cardiomyocytes.

© 2006 Elsevier Inc. All rights reserved.

**Keywords:** Connectin; Titin; Single-molecule; Muscle mechanics; Elasticity; AFM spectroscopy; Protein unfolding; Immunoglobulin domain; Protein kinase A

### 1. Introduction

The molecular basis for the generation of passive-tension and elasticity in vertebrate striated muscle is well-established to be due primarily to the titin filament system (Opitz et al., 2003; Tskhovrebova and Trinick, 2004; Granzier and Labeit, 2004; Prado et al., 2005). Titins, also known as connectins (Maruyama et al., 1976; Wang et al., 1979), constitute a super-family of large elastic muscle proteins ( $M_w$ , 3.0–3.7 MDa) with a highly modular structure. A single titin molecule is in excess of 1  $\mu$ m in length and is composed of up to 300 domains of the immunoglobulin-like (Ig) or fibronectin-like type, interspersed

with unique sequences (Labeit and Kolmerer, 1995). The molecule spans half of a sarcomere, the structural unit of skeletal and cardiac muscle cells, but only the titin segment in the so-called I-band region contributes to muscle elasticity (Fig. 1A) since the remainder is bound firmly to either the thick filament system or the Z-disks (Miller et al., 2004, and references therein).

Single-molecule studies have shown that the elastic properties of titin can be characterized by the sum of several ostensibly independent molecular springs (Li et al., 2002; Leake et al., 2004; Watanabe et al., 2002b). The molecular mechanism of titin elasticity appears to be mainly entropic in nature but an additional component may be due to the unraveling of Ig-domains (Minajeva et al., 2001). Under conditions of high force these domains unfold (Tskhovrebova et al., 1997; 38 39 40 41 42 43 44 45 46 47 48 49 50 51 52 53

\* Corresponding author. Fax: +49 251 8324723.

E-mail address: [wlinke@uni-muenster.de](mailto:wlinke@uni-muenster.de) (W.A. Linke).

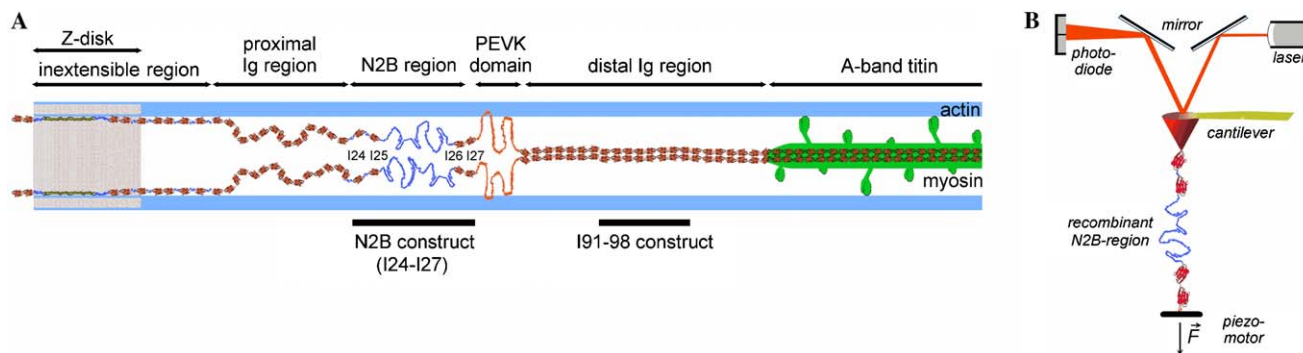


Fig. 1. Atomic force microscope (AFM) force spectroscopy of titin constructs. (A) Schematic of I-band titin domains (N2B-isoform) in the cardiac sarcomere (modified after Neagoe et al. (2003)). Shown are the positions of the recombinant N2B (I24–27) and I91–98 constructs stretched by AFM. (B) Schematic of the AFM setup.

54 Kellermayer et al., 1997; Rief et al., 1997) and in doing  
 55 so may act as shock-absorbers to minimize damage to  
 56 the delicate muscle architecture and allow titin to contin-  
 57 ue a role for passive-tension generation during patho-  
 58 physiological stretch (Agarkova and Perriard, 2005).  
 59 Ig-domain unfolding could also contribute to the visco-  
 60 elastic properties of muscle (Minajeva et al., 2001; Linke  
 61 and Fernandez, 2002; Linke and Leake, 2004). Both single-  
 62 molecule investigations (Rief et al., 1998; Li et al.,  
 63 2002; Watanabe et al., 2002a) and bulk chemical-dena-  
 64 turation studies (Politou et al., 1995) have suggested that  
 65 the stability of Ig-domains may vary over several orders  
 66 of magnitude. When titin-like Ig-domains unfold, they  
 67 also have the potential to refold under substantial forces  
 68 of up to 30 pN (Bullard et al., in press).

69 The so-called N2B-region within I-band titin is a car-  
 70 diac-specific segment containing a large unique sequence  
 71 of 572 amino-acid residues bordered by Ig-domains  
 72 (Fig. 1A). The mechanical characteristics of these Ig-do-  
 73 mains (I24–I27) had been unknown before and were  
 74 studied in the present work. The N2B-unique sequence  
 75 (N2B-U<sub>s</sub>) has earlier been shown to extend towards the  
 76 upper physiological sarcomere length (SL) range, thereby  
 77 contributing to the passive-tension generation of cardiac  
 78 myofibrils (Linke et al., 1999; Helmes et al., 1999).  
 79 Under conditions of cardiac ischemia both the N2B-U<sub>s</sub>  
 80 and the I26/27 Ig-domains of the N2B region associate  
 81 with the chaperone  $\alpha$ -B-crystallin (Bullard et al., 2004).  
 82 Furthermore, the N2B-U<sub>s</sub> binds DRAL/FHL-2, which  
 83 targets metabolic enzymes to the I-band of the cardiac  
 84 sarcomere (Lange et al., 2002). The N2B-U<sub>s</sub> has been  
 85 characterized by single-molecule mechanical studies as  
 86 having different compliance properties to the rest of the  
 87 elastic regions of the titin molecule (Li et al., 2002;  
 88 Watanabe et al., 2002b). There is evidence from myocyte  
 89 studies that the N2B-U<sub>s</sub> can be phosphorylated by pro-  
 90 tein kinase A (Yamasaki et al., 2002), which causes a  
 91 drop in myocardial passive stiffness (van Heerebeek  
 92 et al., in press). Whether the PKA effect on N2B can  
 93 be seen at the single-molecule level in vitro had not yet  
 94 been determined.

Here, we generated a recombinant fragment containing  
 the entire human N2B region, in which the unique  
 sequence is flanked by two Ig-domains on either side  
 (Fig. 1A). The force-extension relationship of the N2B  
 construct was analyzed by single-molecule AFM force spec-  
 troscopy (Fig. 1B) and a possible mechanical effect of  
 PKA-induced phosphorylation was tested. We found that  
 the N2B-U<sub>s</sub> does not extend to the contour length of  
 >200 nm expected from a permanently unfolded entropic  
 spring of 572 residues. This finding, also corroborated by  
 titin extensibility studies on isolated single cardiomyofi-  
 brils, may be explained by the presence of a disulphide  
 bridge within the N2B-U<sub>s</sub>, which was suggested by disul-  
 phide connectivity prediction algorithms. Experimental  
 conditions not matching the environment of titin in muscle  
 cells could be a reason for an observed lack of changes in  
 mechanical properties of the recombinant N2B-construct  
 upon addition of PKA in the presence of ATP.

## 2. Materials and methods

### 2.1. Expression and purification of titin construct

A construct spanning two complete Ig-domains either  
 side of the entire human N2B-region (Lange et al., 2002)  
 was sub-cloned into a pGEX vector with a pEGFP-C1  
 compatible cloning site and inclusive thrombin cleavage  
 site. This construct, I24–27 (Fig. 1), contains the entire  
 human N2B-region plus one additional C-terminal  
 domain, the I27 Ig-domain (formerly called I19 domain)  
 according to the nomenclature by Bang et al. (2001). (Note  
 that we do not use the nomenclature of titin domains after  
 Labeit and Kolmerer (1995), which is often used in single-  
 molecule work!) The pGEX-N2B plasmid was transformed  
 into an *Escherichia coli* expression system generating a  
 GST-N2B fusion of the correct molecular weight (see  
 Fig. 3A). Purification was by a standard Glutathione-  
 Sepharose 4B pull-down assay followed by thrombin  
 cleavage for GST removal. The I91–98 distal Ig-domain  
 construct (Fig. 1A) was kindly donated by Prof. Mathias  
 Gautel (King's College, London).

133 2.2.  $^{32}\text{P}$  autoradiography

134 Phosphorylation of the recombinant N2B-construct was  
 135 probed by standard autoradiography (Witt et al., 2001).  
 136 Briefly, the N2B-construct (1.5 or 2.5  $\mu\text{g}$ ) was incubated  
 137 with the catalytic subunit of protein kinase A (BIAFFIN,  
 138 final concentration 1 U/ $\mu\text{l}$  in 50 mM Tris–HCl pH 7.5,  
 139 10 mM  $\text{MgCl}_2$ , 0.5 mM ATP, 0.06% NaF) in the presence  
 140 of [ $\gamma$ - $^{32}\text{P}$ ]ATP (specific activity, 250  $\mu\text{Ci}/\mu\text{M}$ ) for 60 min at  
 141 30 °C. The protein was then denatured, dissolved, electro-  
 142 phoresed on 10% SDS–polyacrylamide gels, and identified  
 143 by Coomassie-blue staining. The gel was dried and exposed  
 144 to an autoradiographic film for 24 h at room temperature.  
 145  $^{32}\text{P}$ -incorporation was visualized by phosphoimaging  
 146 (Fujifilm BAS-1800 II).

## 147 2.3. AFM force spectroscopy

148 We used a home-built single-molecule atomic force  
 149 microscope (AFM) consisting of a commercial detector  
 150 head (Veeco Instruments, Mannheim, Germany) attached  
 151 to a piezoelectric positioner with strain gauge sensor  
 152 (P841, Physik Instrumente, Karlsruhe, Germany), giving  
 153 a  $z$  axis resolution of a few nm over a measurable force  
 154 range of 10–10,000 pN (Linke et al., 2002; Bullard et al.,  
 155 2004). Force measurement and the control of the move-  
 156 ment of the piezoelectric positioner were achieved by two  
 157 data acquisition boards (PCI 6052E, PCI 6703, National  
 158 Instruments) using custom-written software (LabView;  
 159 National Instruments and Igor, Wavemetrics). The spring  
 160 constant of each individual cantilever (MSCT-AUHW:  
 161 sharpened silicon nitride; Veeco Metrology Group, Santa  
 162 Barbara, CA) was calibrated using the equipartition theo-  
 163 rem (typically  $\sim 40$  pN  $\text{nm}^{-1}$ ). Alternatively, some experi-  
 164 ments were performed using the Asylum Research  
 165 Molecular Force Probe AFM, MFP-3D (Atomic Force  
 166 F&E GmbH, Mannheim, Germany).

167 In a given experiment 50  $\mu\text{l}$  of a 2 nM solution of the rel-  
 168 evant protein were deposited on a freshly coated gold cov-  
 169 erslip (consisting of a 40 nm nickel/chromium base layer  
 170 and 10 nm gold top surface) for 5 min and rinsed with  
 171 PBS (100 mM sodium chloride and 50 mM sodium phos-  
 172 phate, pH 7.0). Mechanical stretch experiments on the  
 173 N2B-construct were performed in the presence or absence  
 174 of protein kinase A (PKA). For the former the coverslip  
 175 was then rinsed by 50  $\mu\text{l}$  of a PKA/ATP solution  
 176 (0.5  $\mu\text{g ml}^{-1}$  PKA, 50  $\mu\text{M}$  ATP in PBS), for the latter  
 177 PBS alone was used. Since some fraction of the PKA mol-  
 178 ecules may bind to the gold, we estimated that the effective  
 179 molar ratio of non-surface-bound PKA to N2B-titin con-  
 180 struct may be  $\sim 5:1$ , with an error of at least 20%. Experi-  
 181 ments on the I91–98 construct were performed in PBS  
 182 alone. Following 5 min for equilibration, segments of the  
 183 proteins were then picked up randomly by adsorption to  
 184 the AFM cantilever tip by pressing down onto the sample  
 185 for 1 s at high force (several nN), and stretching for several  
 186 100 nm. Surface protein density was optimized to ensure a

low probability for tethering to the AFM tip ( $\sim 1$  in 50 187  
 attempts) to minimize the chance for capturing two or 188  
 more molecules and stretching them simultaneously. Such 189  
 events could be seen as overlapping sawtooth patterns 190  
 and readily distinguished from the regularly spaced saw- 191  
 tooth pattern that identified a single-molecule. Experiments 192  
 were performed at a room temperature of 22 °C. The pull- 193  
 ing stretch rate for all force-extension traces usually was 194  
 1  $\mu\text{m s}^{-1}$ . 195

## 2.4. Analysis of force-extension traces 196

Protein elasticity was modeled using the worm-like 197  
 chain (WLC) approach of pure-entropic elasticity (Marko 198  
 and Siggia, 1995) 199

$$F = \left( \frac{k_B T}{L_p} \right) \left[ \frac{1}{4(1 - x/L_c)^2} - \frac{1}{4} + \frac{x}{L_c} \right] \quad 201$$

$F$  is the entropic-based force,  $L_p$  is the persistence length,  $x$  202  
 is end-to-end extension,  $L_c$  is contour length of the 203  
 stretched molecule,  $k_B$  is Boltzmann's constant, and  $T$  is 204  
 absolute temperature. The adjustable parameters were the 205  
 persistence and the contour lengths. Sawtooth force peaks 206  
 were detected by an automated custom-written algorithm 207  
 (LabView), discarding the final force peak in each trace 208  
 as detachment from the coverslip and/or AFM tip. Contin- 209  
 uous inter-peak segments of each force-extension trace 210  
 were then fitted by a WLC, using a convergence tolerance 211  
 of 1 nm for  $L_c$  and 0.05 nm for  $L_p$ . If the difference in  $L_c$  212  
 for adjacent segments fell within the range 24–32 nm for 213  
 a given fixed  $L_p$  then the force peak of the preceding seg- 214  
 ment was assigned as an Ig-domain unfolding event (Rief 215  
 et al., 1997; Li et al., 2002). 216

2.5. Disulphide connectivity prediction for the human 217  
 N2B-unique sequence 218

Disulphide bonds in the N2B-Us were predicted with 219  
 two different novel algorithms. The DiANNA (DiAmino- 220  
 acid Neural Network Application) web-server ([http:// 221](http://clavius.bc.edu/~clotelab/DiANNA/)  
[clavius.bc.edu/~clotelab/DiANNA/](http://clavius.bc.edu/~clotelab/DiANNA/)) runs a disulphide 222  
 connectivity algorithm utilizing a novel architecture neural 223  
 network. A diresidue Neural Network (Ferre and Clote, 224  
 2005) is trained to recognize pairs of bonded half-cysteines 225  
 given input of half-cysteines symmetric flanking regions. 226  
 The network-training uses disulphide bond information 227  
 derived from high-quality protein structures (Vullo and 228  
 Frascioni, 2004), including evolutionary as well as second- 229  
 ary structure information. A running window PSIPRED 230  
 is first performed on the whole input sequence to predict 231  
 the secondary structure (helix, coil, and sheet) followed 232  
 by PSIBLAST to produce the profile of each position with- 233  
 in the running window (Jones, 1999). 234

The DISULFIND web-server ([http://cassandra.dsi.uni- 235](http://cassandra.dsi.uni-fi.it/disulfind)  
[fi.it/disulfind](http://cassandra.dsi.uni-fi.it/disulfind)) employs an SVM binary classifier to predict 236  
 the bonding state of each cysteine (Ceroni et al., 2003), 237



238 followed by a refinement stage that collectively classifies all  
 239 the cysteines in the chain. A bidirectional recurrent neural  
 240 network (BRNN), similar to DiANNA, and a Viterbi  
 241 decoder finds the maximum likelihood bonding state  
 242 assignment which satisfies the constraint for having an even  
 243 number of disulphide bonded cysteines (ignoring inter-  
 244 chain bonds).

### 245 3. Results

#### 246 3.1. Expression and phosphorylation of the human N2B-titin 247 construct, I24–27

248 The full-length N2B-region of human cardiac titin contain-  
 249 ing the N2B-U<sub>s</sub> and three Ig-domains, plus the I27-do-  
 250 main (Fig. 1), was expressed in *E. coli* generating a GST-  
 251 N2B fusion of the correct molecular weight (Fig. 2A).  
 252 The construct could be readily phosphorylated by the cat-  
 253 alytic subunit of PKA in the presence of ATP, as demon-  
 254 strated by autoradiography (Fig. 2B).

#### 255 3.2. Mechanical stability of Ig-domains in the human 256 N2B-titin construct, I24–27

257 Stretching of the N2B-construct resulted in sawtooth  
 258 force-extension traces (Figs. 3A–C) containing up to four  
 259 clear force peaks (excluding the final detachment peak).  
 260 Modeling of the inter-peak force-extension segments sug-  
 261 gested most could be characterized by a WLC of persis-  
 262 tence length,  $L_p$ ,  $\sim 0.2$ – $0.4$  nm, with a characteristic  
 263 spacing in contour length,  $L_c$ , between adjacent segments  
 264 of  $\sim 30$  nm (Figs. 3A and B).

265 PKA-dependent phosphorylation of the N2B-region  
 266 presumably alters titin's mechanical properties (Yamasaki  
 267 et al., 2002) and though this effect is thought to be medi-  
 268 ated by the N2B-U<sub>s</sub>, we tested whether PKA indeed leaves  
 269 the Ig-domains of the N2B-segment unaffected. A compar-  
 270 ison of sawtooth patterns at equivalent rates of stretch  
 271 showed no consistent changes in the unfolding force ( $F_u$ )

of Ig-domains upon addition of PKA in the presence of  
 ATP (Figs. 3A–C). Comparing just the second force peak  
 putatively assigned to unfolding of the same Ig-domain  
 suggested that PKA does not significantly alter the force  
 required to unfold this domain (mean  $F_u$ , 220–235 pN;  
 Fig. 4A). Histograms of unfolding forces (all peaks)  
 showed no difference in the mean  $F_u$ , in the absence  
 ( $F_u = 218 \pm 18$  pN) and presence ( $F_u = 228 \pm 15$  pN) of  
 PKA (Figs. 4C and D).

The mechanical properties of the Ig-domains in the  
 N2B-construct were compared to those of a well-studied  
 recombinant Ig-domain construct, I91–98 (elsewhere  
 named I27–34; e.g., Rief et al., 1997; Li et al., 2002),  
 from the distal Ig-domain region (Fig. 1). Stretching this  
 construct (in PBS) resulted in sawtooth force-extension  
 traces containing between two and seven detected force  
 peaks (Fig. 3D). WLC modeling again suggested that  
 post-Ig-unfold elastic regions of the traces can be charac-  
 terized by a persistence length,  $L_p$ , of  $\sim 0.2$  nm with a  
 characteristic spacing in contour length,  $L_c$ , between  
 adjacent segments of  $\sim 28$  nm. The Ig-domain unfolding  
 force for just the second force peak at stretch rate  
 $1 \mu\text{m s}^{-1}$  had a mean value of 230 pN (Fig. 4A) and  
 the mean  $F_u$  for all detected force peaks was 244 pN  
 (Fig. 4B).

#### 3.3. Mechanical properties of the N2B-unique sequence with and without PKA

Sawtooth traces of the N2B-construct containing three  
 to four regularly spaced unfolding peaks were analyzed  
 to parameterize the mechanical properties of the N2B-U<sub>s</sub>  
 (Figs. 3A–C). Modeling the initial trace leading up to the  
 first unfolding peak—presumably corresponding to the  
 stretching of the whole N2B-U<sub>s</sub>—resulted in WLC fits with  
 $L_p$  between 0.40 and 0.70 nm (in PBS), though the frequent  
 appearance of initial force bumps due to rupture of multi-  
 molecular adhesions to the cantilever tip (e.g., Fig. 3B)  
 made the analysis less reliable. Upon addition of PKA

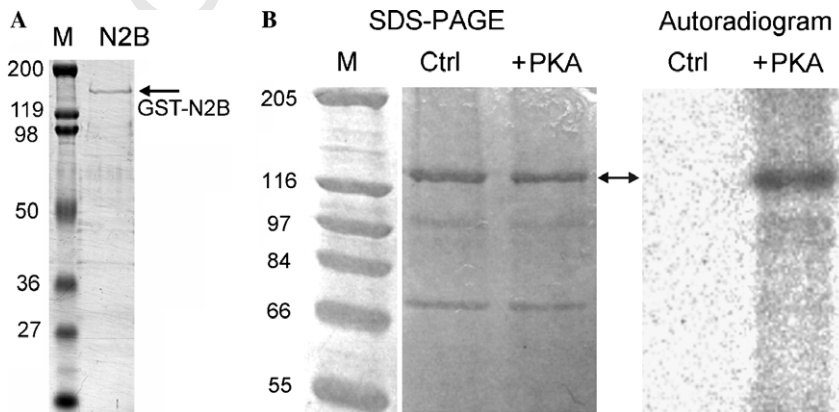


Fig. 2. Expression and phosphorylation of the recombinant N2B-construct (I24–27). (A) SDS-gel electrophoresis of purified GST-N2B product (lane 2) compared against molecular weight markers (lane 1), values marked in kDa. (B) Autoradiography detects phosphorylation of the N2B-construct by catalytic subunit of protein kinase A (PKA) in the presence of ATP. Ctrl, no PKA added. Lanes were loaded with 2.5  $\mu\text{g}$  (Ctrl) and 1.5  $\mu\text{g}$  (+PKA) protein. M, size marker.

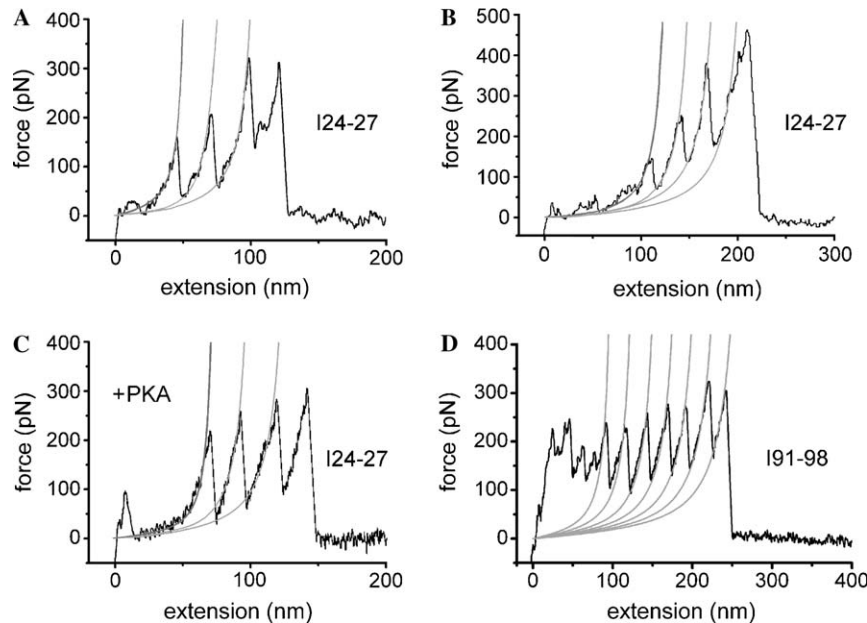


Fig. 3. Force-extension recordings for the recombinant N2B-construct (I24-27), in comparison to an Ig-domain only construct (I91-98). The N2B-construct was stretched in PBS (A) and (B) or in PBS plus PKA in the presence of ATP (C). Unfolding forces were compared to those measured at equivalent stretch rates ( $1 \mu\text{m s}^{-1}$ ) for the I91-98 construct (D). Grey curves are worm-like chain fits to the sawtooth peaks (dark grey indicates fit to the first force maximum in A-C). The constant contour-length increment between peaks hints at the presence of single-molecule tethers.

309 the range of persistence length for the initial WLC fit was  
310 unchanged at 0.30–0.60 nm.

311 Datasets measuring the origin-to-first-peak force-extension  
312 segment suggested a comparable mean contour length  
313 for the N2B-U's of  $L_c \sim 120$  nm, for stretches in both the  
314 presence and absence of PKA (Fig. 4E). Histogram analyses  
315 for  $L_c$  showed a major peak at  $\sim 95$  nm under both  
316 experimental conditions (Figs. 4F and G). However, there  
317 was an additional minor peak centered around 180 nm for  
318 N2B-U's stretched in PBS only (Fig. 4F), and a substantial  
319 number of long  $L_c$ -values up to 240 nm appeared when  
320 N2B-U's was stretched in the presence of PKA (Fig. 4G).  
321 A predominant contour length of 90–100 nm is lower than  
322 what might be expected from sequence data alone, based  
323 on a putative random-coil of 572 residues.

#### 324 3.4. Limited extensibility of the N2B-unique sequence in 325 cardiac myofibrils

326 To follow up on this point, we compared the  $L_c$  of the  
327 N2B-U's measured by AFM force spectroscopy with the  
328 maximum extension of that titin segment determined by  
329 immunostaining methods on myofibrils (Fig. 5). Two different  
330 anti-titin antibodies directly flanking the N2B-U's  
331 (I25, I26; Fig. 5A) have been used by us previously to stain  
332 cardiac sarcomeres at different degrees of stretch (the anti-  
333 bodies were formerly named I17 and I18, respectively;  
334 Linke et al., 1999) and to obtain the SL-dependent transla-  
335 tional mobility of both antibody epitopes (Figs. 5B and C).  
336 Here, we compiled data from Linke et al. (1999) and  
337 extended the analysis to the highly stretched SLs to calcu-  
338 late the maximum extension of the full N2B-U's in the

sarcomere up to a length of  $\sim 2.9 \mu\text{m}$  (Fig. 5C, inset). At  
the longer SLs the extension of the N2B-U's leveled out  
at  $\sim 100$  nm, suggesting that also in situ this region extends  
to a contour length lower than expected from a permanent-  
ly unfolded random-coil.

#### 344 4. Discussion

345 Single-molecule AFM force spectroscopy has been used  
346 for almost a decade to help establish the mechanical behav-  
347 ior of individual domains of the giant muscle protein titin  
348 (e.g., Rief et al., 1997, 1998; Carrion-Vazquez et al.,  
349 1999; Li et al., 2002; Watanabe et al., 2002b; Scott et al.,  
350 2002). Various I-band titin domains have been analyzed,  
351 particularly those from the proximal and distal Ig-domain  
352 segments (Fig. 1A), and also the PEVK-domain is mechan-  
353 ically well-studied at the single-molecule level (Li et al.,  
354 2001, 2002; Linke et al., 2002; Watanabe et al., 2002b;  
355 Leake et al., 2004; Nagy et al., 2005). In contrast, less is  
356 known about the cardiac-specific N2B-region (Fig. 1A),  
357 of which only the unique sequence was investigated previ-  
358 ously by single-molecule AFM (Li et al., 2002; Watanabe  
359 et al., 2002b). Here, we cloned a recombinant fragment  
360 containing the full N2B-region and used AFM force spec-  
361 troscopy to measure the mechanical characteristics of the  
362 N2B-U's as well as the Ig-domains. Comparing the Ig-do-  
363 main stabilities of the N2B-region with those of a recombi-  
364 nant fragment of distal Ig-domains (I91-98) at equivalent  
365 rates of stretch, we found similar unfolding forces (mean,  
366  $\sim 220$ – $240$  pN). Further, the N2B-specific Ig-domains  
367 showed a rather large range of unfolding forces  
368 (100–400 pN) comparable to those found among distal

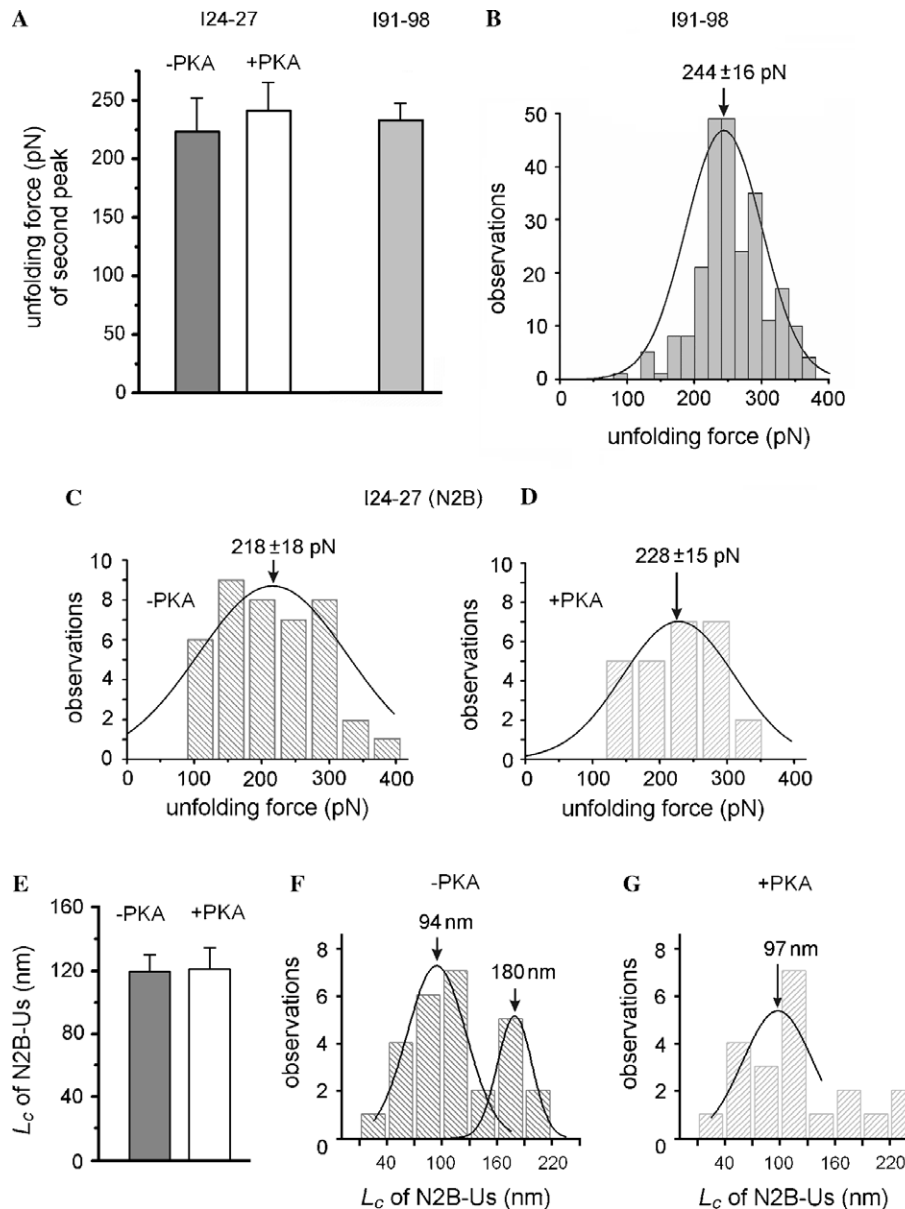


Fig. 4. Mechanical properties of the N2B-region. (A) Ig-domain unfolding forces of the second force peak, collated at a stretch rate of  $1 \mu\text{m s}^{-1}$  for the N2B-construct (I24–27) in the absence and presence of PKA (left two columns), and the I91–98 construct in PBS only (right column). Numbers in each dataset are 14, 11, and 131 (from left to right). Error bars are one SE. (B) Histogram of unfolding forces (all peaks) for the I91–98 construct and Gaussian fit. (C) Unfolding force histogram and Gaussian fit for peaks of N2B-Ig-domains in the absence of PKA. (D) The same, but in the presence of PKA. (E) Mean contour length ( $L_c$ ) of the N2B-U.s calculated from WLC fits of the segment between zero and the first force peak, in the absence ( $n = 27$ ) and presence ( $n = 21$ ) of PKA. Values in (B–E) are mean  $\pm$  SE. (F) Histogram of contour-lengths values for the N2B-construct in PBS and Gaussian fits showing a major center around 94 nm and a minor center around 180 nm. (G) The same, but for N2B in PKA + ATP.

369 Ig-domains (Rief et al., 1997; Li et al., 2001; Watanabe  
370 et al., 2002a). Thus, the Ig-domains of the N2B-region  
371 are mechanically similar to other Ig-domains in titin.

372 The wide interest in the unfolding characteristics of titin  
373 Ig-domains notwithstanding, it is still controversial  
374 whether or not these domains unfold in muscle sarcomeres  
375 (Minajeva et al., 2001; Trombitas et al., 2003; Linke and  
376 Leake, 2004). Based on the observation of higher mechanical  
377 stability of distal Ig-domains compared to proximal  
378 domains (Li et al., 2002), it is likely that the distal Ig-do-  
379 mains do not unfold in situ (Linke et al., 1999; Tskhovreb-  
380 ova and Trinick, 2001; Linke and Fernandez, 2002). The

high mean stability of the N2B-specific Ig-domains found 381  
here suggests that most of these domains may remain fold- 382  
ed during normal cardiac function as well. However, with 383  
some Ig-domains in the N2B-region unfolding at forces 384  
as low as 100 pN at a stretch rate of  $1 \mu\text{m s}^{-1}$ , it cannot 385  
be excluded that a few of these domains do unfold in the 386  
sarcomere during high physiological stretch, as suggested 387  
earlier for the proximal Ig-domains (Linke et al., 1999; 388  
Linke and Fernandez, 2002; Li et al., 2002; Bullard et al., 389  
2004). 390

Studying the mechanical characteristics of the N2B-U.s 391  
bordered by the naturally flanking Ig-domains, we collect- 392



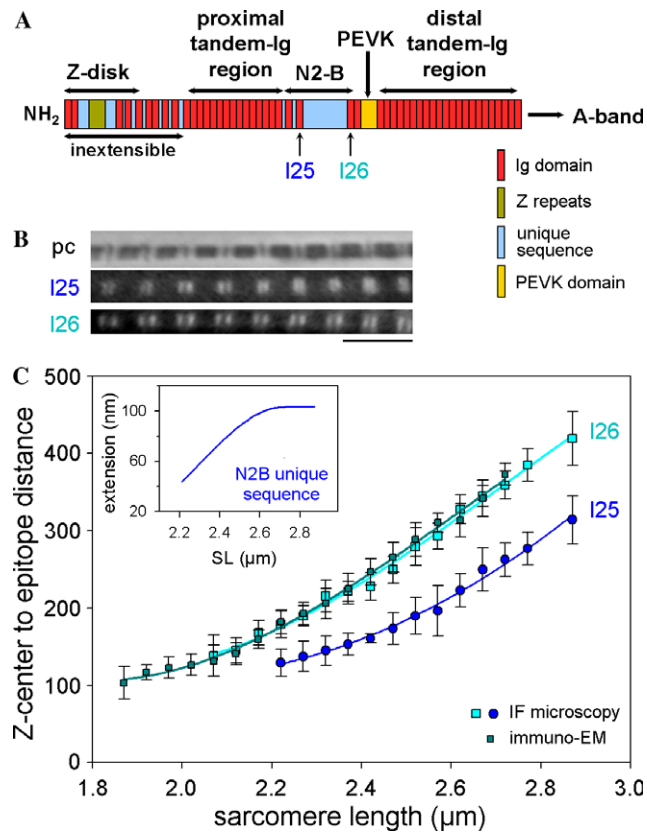


Fig. 5. Extensibility of the N2B-U region in rabbit cardiac myofibrils. (A) Schematic view of the domain architecture of the elastic region of the cardiac N2B-titin isoform (after Labeit and Kolmerer, 1995). Epitope locations of anti-titin antibodies (I25 and I26) flanking the N2B-U region, which were used for immunostaining experiments, are indicated by arrows. (B) Immunofluorescence images of single cardiac myofibrils stretched in relaxing buffer and labeled with the two different antibodies at SL 2.7  $\mu\text{m}$ . pc, Phase image; bar, 5  $\mu\text{m}$ . (C) Distance between Z line center and nearest antibody epitope for a large range of SLs, measured by immunofluorescence (IF) and immunoelectron microscopy. Data were compiled from Linke et al. (1999) and some points were added for SL  $\sim$ 2.9  $\mu\text{m}$ . Symbols are means  $\pm$  SD, fits are three-order regressions. (Inset) Stretch-dependent extension of the N2B-U region in the sarcomere. Note the distinct plateau at SL  $<$  2.6  $\mu\text{m}$  showing a maximum extension of  $\sim$ 100 nm.

ed evidence that this unique sequence may not behave as a permanently unfolded, putative random-coil segment, contrary to previous belief (Li et al., 2002; Watanabe et al., 2002b). The mean contour length of the N2B-U region (120 nm) reached much less than the 220 nm expected from a random-coil of 572 residues. Elsewhere, mean contour-length values above 200 nm were observed in single-molecule AFM studies using the N2B-U region alone (Watanabe et al., 2002b) or the N2B-U region flanked by rows of I91 Ig-domains (Li et al., 2002). In our hands, there was a bimodal distribution of contour-length values with two centers at 90–100 nm (major peak) and  $\sim$ 180 nm (minor peak). In an attempt to explain this unexpected finding, we considered the possibility that there could be some intramolecular structuring within the unique sequence, more specifically an S–S bond between the cysteines (the human N2B-U region has six cysteines; Labeit and Kolmerer, 1995) which the AFM cannot break. Two different web-based algorithms,

DiANNA and DISULFIND (see Section 2), were used for disulphide connectivity prediction.

Surprisingly, a high propensity for disulphide bridge formation was suggested by both algorithms, although results differed with regard to the position of the bond (Fig. 6A). DISULFIND predicted connectivity between cysteines in position seven (confidence eight out of nine) and position 100 (confidence four out of nine) in the 572-residue human N2B-U region, whereas DiANNA predicted bonding between cysteines 100 and 445 (probability, 0.961); all other cysteines are unlikely to be bonded (Fig. 6A). An S–S bridge between residues 7 and 100 would suggest that the “free” bit of the N2B-U region stretched has a contour length of  $\sim$ 0.38 nm  $\times$  480 =  $\sim$ 180 nm. If the S–S were between residues 100 and 445, the free contour length would be 0.38 nm  $\times$  227 =  $\sim$ 90 nm (Fig. 6B). Although, it could just be coincidental, it is remarkable that these contour-length values exactly match the mean values of the two populations for  $L_c$  found by us.

Why our  $L_c$  values differ from those reported in previous studies (Li et al., 2002; Watanabe et al., 2002b) remains unknown at this stage. Possibly, different conditions during protein expression contribute to the disparity and one can also speculate that the differences may be a consequence of us using the whole “native” N2B-U region, including the naturally flanking Ig-domains. When we measured the extensibility of the N2B-U region in the natural setting of the cardiac myofibril, this titin segment extended to no more than  $\sim$ 100 nm even under extreme stretch (Fig. 5). Elsewhere, the N2B-U region could be stretched maximally to  $\sim$ 150 nm in the environment of the sarcomere (Trombitas et al., 1999). Perhaps an important methodological difference between our data and those of Trombitas et al. (1999) is that these authors used reducing agent (DTT, 1 mM) in their relaxing buffer, unlike us (cf., Linke et al., 1999). Inside the muscle cells there is a reducing environment due mainly to the presence of glutathione (GSH) (Rutten et al., 2005) and normally the formation of disulphide bridges is unlikely. However, it is possible that the extensibility and spring force of the N2B-U region are modified under conditions that favor the oxidized state—a scenario that has been proposed also for some titin Ig-domains potentially containing an internal disulfide bridge (Mayans et al., 2001). Whether the redox state indeed modifies the mechanical properties of the N2B-U region is testable in future work both at the single-molecule level and in myofibrils.

Of particular interest in this study was the effect of protein kinase A on the mechanical characteristics of the N2B-U region. The addition of PKA (in the presence of ATP) to cardiac myocytes has been shown to decrease passive stiffness (Yamasaki et al., 2002; van Heerebeek et al., in press) and also  $\beta$ -adrenergic stimulation has, via PKA, a softening effect on resting cardiac muscle (Fukuda et al., 2005). These effects have been explained by PKA-aided phosphorylation of titin’s N2B-U region (Yamasaki et al., 2002), although no molecular mechanism is currently known to satisfactorily explain how phosphorylation of this region could

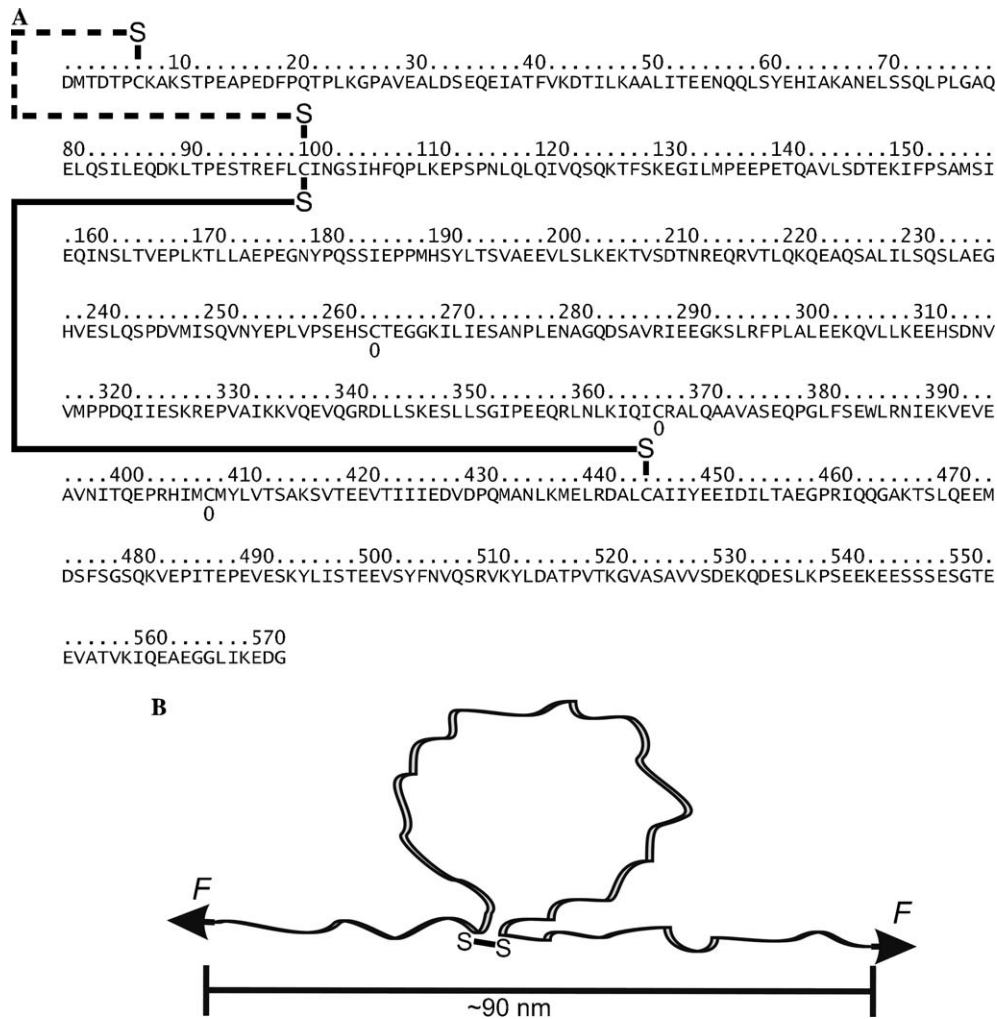


Fig. 6. Disulphide connectivity predictions for the N2B-unique sequence. (A) Sequence of the N2B-Us; residues 1–572 are equivalent to residues 3671–4242 of the human cardiac titin N2B-isoform (Accession No. X90568 in GenBank™/EBI Data Bank). The output by the DISULFIND (<http://cassandra.dsi.unifi.it/disulfind>) and DiANNA (<http://clavius.bc.edu/~clotelab/DiANNA/>) algorithms is shown, suggesting connectivity between cysteines in positions 7 and 100 (dashed line) or in positions 100 and 445 (solid line), respectively. “0” indicates not-bonded cysteine. (B) Schematic of the N2B-Us with a suggested free contour length of ~90 nm if there were a bond between cysteines 100 and 445.

468 modify titin stiffness. We searched for a direct effect of  
 469 PKA + ATP on the force-extension behavior of the N2B-  
 470 titin fragment at the single-molecule level, but found none.  
 471 Neither the Ig-domain stability nor the contour length/per-  
 472 sistence length of the N2B-Us appeared to be affected by  
 473 PKA. A possible explanation is that PKA + ATP alone  
 474 is not sufficient to lower N2B stiffness. The kinase,  
 475 although capable of phosphorylating the N2B-region,  
 476 might need one or more co-factor(s) to trigger the de-stiff-  
 477 ening in cardiac cells. Our results also hint at the possibility  
 478 that the PKA effect may require reducing conditions. Addi-  
 479 tional work is needed to establish a molecular mechanism  
 480 of PKA action on titin.

481 In summary, we conclude the following about the  
 482 mechanical properties of titin’s N2B-region. (1) The Ig-do-  
 483 mains in this region are mechanically similar to other  
 484 I-band titin domains. (2) The mean contour length of the  
 485 N2B-unique sequence reached much less than the  
 486 ~220 nm expected for a fully stretched random-coil of

572 residues, suggesting that this titin segment does not  
 487 behave as a permanently unfolded entropic spring; the find-  
 488 ing might be explainable by the formation of a disulphide  
 489 bridge under non-reducing conditions. (3) Limited extensi-  
 490 bility of the N2B-Us was detected also in isolated, highly  
 491 stretched, cardiac sarcomeres; possibly then, the N2B  
 492 spring stiffness is increased under oxidative stress condi-  
 493 tions. (4) There was no direct effect of PKA in the presence  
 494 of ATP on the mechanical characteristics of the recombi-  
 495 nant N2B-region, although phosphorylation was  
 496 detectable.  
 497

#### Acknowledgments

498  
 499 We thank Prof. Julio Fernandez and Dr. Hongbin Li  
 500 (Columbia University, New York) for advice in developing  
 501 the AFM force spectroscopy apparatus. We are grateful to  
 502 Dr. Stephan Lange (King’s College London) for donating  
 503 the original pGEX-DRAL vector for the N2B-construct



504 and to Dr. Bogos Agianian (EMBL Heidelberg) for the  
505 bacterial transformation and final peptide purification.  
506 The I91–98 construct was a kind donation of Prof. Mathias  
507 Gautel (King's College London). We acknowledge finan-  
508 cial support of the Deutsche Forschungsgemeinschaft  
509 (SFB 629, TP10 to W.A.L.).

## 510 References

- 511 Agarkova, I., Perriard, J.C., 2005. The M-band: an elastic web that  
512 crosslinks thick filaments in the center of the sarcomere. *Trends Cell*  
513 *Biol.* 15, 477–485.
- 514 Bang, M.L., Centner, T., Fornoff, F., Geach, A.J., Gotthardt, M.,  
515 McNabb, M., Witt, C.C., Labeit, D., Gregorio, C.C., Granzier, H.,  
516 Labeit, S., 2001. The complete gene sequence of titin expression of an  
517 unusual approximately 700-kDa titin isoform and its interaction with  
518 obscurin identify a novel Z-line to I-band linking system. *Circ. Res.* 89,  
519 1065–1072.
- 520 Bullard, B., Benes, V., Garcia, T., Leake, M.C., Linke, W.A., Oberhauser,  
521 A.F., in press. The molecular elasticity of the insect flight muscle  
522 proteins projectin and kettin. *Proc. Natl. Acad. Sci. USA*.
- 523 Bullard, B., Ferguson, C., Minajeva, A., Leake, M.C., Gautel, M., Labeit,  
524 D., Ding, L., Labeit, S., Horwitz, J., Leonard, K.R., Linke, W.A.,  
525 2004. Association of the chaperone alphaB-crystallin with titin in heart  
526 muscle. *J. Biol. Chem.* 279, 7917–7924.
- 527 Carrion-Vazquez, M., Oberhauser, A.F., Fowler, S.B., Marszalek, P.E.,  
528 Broedel, S.E., Clarke, J., Fernandez, J.M., 1999. Mechanical and  
529 chemical unfolding of a single protein: a comparison. *Proc. Natl.*  
530 *Acad. Sci. USA* 96, 3694–3699.
- 531 Ceroni, A., Frascioni, P., Passerini, A., Vullo, A., 2003. Predicting the  
532 disulfide bonding state of cysteines with combinations of kernel  
533 machines. *J. VLSI Signal Proc.* 35, 287–295.
- 534 Ferre, F., Clote, P., 2005. Disulfide connectivity prediction using  
535 secondary structure information and diresidue frequencies. *Bioinforma-*  
536 *tics* 21, 2336–2346.
- 537 Fukuda, N., Wu, Y., Nair, P., Granzier, H.L., 2005. Phosphorylation of  
538 titin modulates passive stiffness of cardiac muscle in a titin isoform-  
539 dependent manner. *J. Gen. Physiol.* 125, 257–271.
- 540 Granzier, H.L., Labeit, S., 2004. The giant protein titin: a major player in  
541 myocardial mechanics, signaling, and disease. *Circ. Res.* 94, 284–295.
- 542 Helmes, M., Trombitas, K., Centner, T., Kellermayer, M., Labeit, S.,  
543 Linke, W.A., Granzier, H., 1999. Mechanically driven contour-length  
544 adjustment in rat cardiac titin's unique N2B sequence: titin is an  
545 adjustable spring. *Circ. Res.* 84, 1339–1352.
- 546 Jones, D.T., 1999. Protein secondary structure prediction based on  
547 position-specific scoring matrices. *J. Mol. Biol.* 292, 195–202.
- 548 Kellermayer, M.S.Z., Smith, S.B., Granzier, H.L., Bustamante, C., 1997.  
549 Folding–unfolding transitions in single titin molecules characterized  
550 with laser tweezers. *Science* 276, 1112–1116.
- 551 Labeit, S., Kolmerer, B., 1995. Titins, giant proteins in charge of muscle  
552 ultrastructure and elasticity. *Science* 270, 293–296.
- 553 Lange, S., Auerbach, D., McLoughlin, P., Perriard, E., Schafer, B.W.,  
554 Perriard, J.C., Ehler, E., 2002. Subcellular targeting of metabolic  
555 enzymes to titin in heart muscle may be mediated by DRAL/FHL-2. *J.*  
556 *Cell Sci.* 115, 4925–4936.
- 557 Leake, M.C., Wilson, D., Gautel, M., Simmons, R.M., 2004. The elasticity  
558 of single titin molecules using a two-bead optical tweezers assay.  
559 *Biophys. J.* 87, 1112–1135.
- 560 Li, H., Oberhauser, A.F., Redick, S.D., Carrion-Vazquez, M., Erickson,  
561 H.P., Fernandez, J.M., 2001. Multiple conformations of PEVK  
562 proteins detected by single-molecule techniques. *Proc. Natl. Acad.*  
563 *Sci. USA* 98, 10682–10686.
- 564 Li, H., Linke, W.A., Oberhauser, A.F., Carrion-Vazquez, M.,  
565 Kerkvliet, J.G., Lu, H., Marszalek, P.E., Fernandez, J.M., 2002.  
566 Reverse engineering of the giant muscle protein titin. *Nature* 418,  
567 998–1002.
- Linke, W.A., Fernandez, J.M., 2002. Cardiac titin: molecular basis of  
568 elasticity and cellular contribution to elastic and viscous stiffness  
569 components in myocardium. *J. Muscle Res. Cell Motil.* 23, 483–497.  
570
- Linke, W.A., Leake, M.C., 2004. Multiple sources of passive stress  
571 relaxation in muscle fibers. *Phys. Med. Biol.* 49, 3613–3627.  
572
- Linke, W.A., Kulke, M., Li, H., Fujita-Becker, S., Neagoe, C., Manstein,  
573 D.J., Gautel, M., Fernandez, J.M., 2002. PEVK domain of titin: an  
574 entropic spring with actin-binding properties. *J. Struct. Biol.* 137, 194–  
575 205.
- Linke, W.A., Rudy, D.E., Centner, T., Gautel, M., Witt, C., Labeit, S.,  
576 Gregorio, C.C., 1999. I-band titin in cardiac muscle is a three-element  
577 molecular spring and is critical for maintaining thin filament structure.  
578 *J. Cell Biol.* 146, 631–644.
- Marko, J.F., Siggia, E.D., 1995. Stretching DNA. *Macromolecules* 28,  
581 8759–8770.
- Maruyama, K., Natori, R., Nonomura, Y., 1976. New elastic protein from  
582 muscle. *Nature* 262, 58–60.
- Mayans, O., Wuerges, J., Canela, S., Gautel, M., Wilmanns, M., 2001.  
583 Structural evidence for a possible role of reversible disulphide bridge  
584 formation in the elasticity of the muscle protein titin. *Structure*  
585 (Camb.) 9, 331–340.
- Miller, M.K., Granzier, H., Ehler, E., Gregorio, C.C., 2004. The sensitive  
586 giant: the role of titin-based stretch sensing complexes in the heart.  
587 *Trends Cell Biol.* 14, 119–126.
- Minajeva, A., Kulke, M., Fernandez, J.M., Linke, W.A., 2001. Unfolding  
588 of titin domains explains the viscoelastic behavior of skeletal myofi-  
589 brils. *Biophys. J.* 80, 1442–1451.
- Nagy, A., Grama, L., Huber, T., Bianco, P., Trombitas, K., Granzier,  
590 H.L., Kellermayer, M.S., 2005. Hierarchical extensibility in the PEVK  
591 domain of skeletal-muscle titin. *Biophys. J.* 89, 329–336.
- Neagoe, C., Opitz, C.A., Makarenko, I., Linke, W.A., 2003. Gigantic  
592 variety: expression patterns of titin isoforms in striated muscles and  
593 consequences for myofibrillar passive stiffness. *J. Muscle Res. Cell*  
594 *Motil.* 24, 175–189.
- Opitz, C.A., Kulke, M., Leake, M.C., Neagoe, C., Hinssen, H., Hajjar,  
595 R.J., Linke, W.A., 2003. Damped elastic recoil of the titin spring in  
596 myofibrils of human myocardium. *Proc. Natl. Acad. Sci. USA* 100,  
597 12688–12693.
- Politou, A.S., Thomas, D.J., Pastore, A., 1995. The folding and stability of  
598 titin immunoglobulin-like modules, with implications for the mecha-  
599 nism of elasticity. *Biophys. J.* 69, 2601–2610.
- Prado, L., Makarenko, I., Andresen, C., Krüger, M., Opitz, C.A., Linke,  
600 W.A., 2005. Isoform diversity of giant proteins in relation to passive  
601 and active contractile properties of rabbit skeletal muscles. *J. Gen.*  
602 *Physiol.* 126, 461–480.
- Rief, M., Gautel, M., Oesterhelt, F., Fernandez, J.M., Gaub, H.E., 1997.  
603 Reversible unfolding of individual titin immunoglobulin domains by  
604 AFM. *Science* 276, 1109–1112.
- Rief, M., Gautel, M., Schemmel, A., Gaub, H.E., 1998. The mechanical  
605 stability of immunoglobulin and fibronectin III domains in the muscle  
606 protein titin measured by atomic force microscopy. *Biophys. J.* 75,  
607 3008–3014.
- Rutten, E.P., Engelen, M.P., Schols, A.M., Deutz, N.E., 2005. Skeletal  
608 muscle glutamate metabolism in health and disease: state of the art.  
609 *Curr. Opin. Clin. Nutr. Metab. Care* 8, 41–51.
- Scott, K.A., Steward, A., Fowler, S.B., Clarke, J., 2002. Titin; a  
610 multidomain protein that behaves as the sum of its parts. *J. Mol.*  
611 *Biol.* 315, 819–829.
- Trombitas, K., Freiburg, A., Centner, T., Labeit, S., Granzier, H., 1999.  
612 Molecular dissection of N2B cardiac titin's extensibility. *Biophys. J.*  
613 77, 3189–3196.
- Trombitas, K., Wu, Y., McNabb, M., Greaser, M., Kellermayer, M.S.,  
614 Labeit, S., Granzier, H., 2003. Molecular basis of passive stress  
615 relaxation in human soleus fibers: assessment of the role of immuno-  
616 globulin-like domain unfolding. *Biophys. J.* 85, 3142–3153.
- Tskhovrebova, L., Trinick, J., 2001. Flexibility and extensibility in the titin  
617 molecule: analysis of electron microscope data. *J. Mol. Biol.* 310, 755–  
618 771.

- 636 Tskhovrebova, L., Trinick, J., 2004. Properties of titin immunoglobulin  
637 and fibronectin-3 domains. *J. Biol. Chem.* 279, 46351–46354.
- 638 Tskhovrebova, L., Trinick, J., Sleep, J.A., Simmons, R.M., 1997. Elasticity  
639 and unfolding of single molecules of the giant muscle protein titin.  
640 *Nature* 387, 308–312.
- 641 van Heerebeek, L., Borbély, A., Niessen, H.W.M., Bronzwaer, J.G.F., van  
642 der Velden, J., Stienen, G.J., Linke, W.A., Laarman, G.J., Paulus,  
643 W.J., in press. Myocardial structure and function differ in systolic and  
644 diastolic heart failure. *Circulation*.
- 645 Vullo, A., Frasconi, P., 2004. Disulfide connectivity prediction using  
646 recursive neural networks and evolutionary information. *Bioinformatics*  
647 20, 653–659.
- 648 Wang, K., McClure, J., Tu, A., 1979. Titin: major myofibrillar  
649 component of striated muscle. *Proc. Natl. Acad. Sci. USA* 76,  
650 3698–3702.
- Watanabe, K., Muhle-Goll, C., Kellermayer, M.S., Labeit, S., Granzier, H., 2002a. Different molecular mechanics displayed by titin's constitutively and differentially expressed tandem Ig segments. *J. Struct. Biol.* 137, 248–258.
- Watanabe, K., Nair, P., Labeit, D., Kellermayer, M.S., Greaser, M., Labeit, S., Granzier, H., 2002b. Molecular mechanics of cardiac titin's PEVK and N2B spring elements. *J. Biol. Chem.* 277, 11549–11558.
- Witt, C.C., Gerull, B., Davies, M.J., Centner, T., Linke, W.A., Thierfelder, L., 2001. Hypercontractile properties of cardiac muscle fibers in a knock-in mouse model of cardiac myosin-binding protein-C. *J. Biol. Chem.* 276, 5353–5359.
- Yamasaki, R., Wu, Y., McNabb, M., Greaser, M., Labeit, S., Granzier, H., 2002. Protein kinase A phosphorylates titin's cardiac-specific N2B domain and reduces passive tension in rat cardiac myocytes. *Circ. Res.* 90, 1181–1188.

UNCORRECTED PROOF